

Organic & Biomolecular Chemistry

Accepted Manuscript



This article can be cited before page numbers have been issued, to do this please use: Y. ye, B. Zhang, R. Mao, C. Zhang, Y. Wang, J. Xing, Y. Liu, X. Luo, H. Ding, Y. Yang, B. Zhou, H. Jiang, K. Chen, C. Luo and M. Zheng, *Org. Biomol. Chem.*, 2017, DOI: 10.1039/C7OB00070G.



This is an Accepted Manuscript, which has been through the Royal Society of Chemistry peer review process and has been accepted for publication.

Accepted Manuscripts are published online shortly after acceptance, before technical editing, formatting and proof reading. Using this free service, authors can make their results available to the community, in citable form, before we publish the edited article. We will replace this Accepted Manuscript with the edited and formatted Advance Article as soon as it is available.

You can find more information about Accepted Manuscripts in the [author guidelines](#).

Please note that technical editing may introduce minor changes to the text and/or graphics, which may alter content. The journal's standard [Terms & Conditions](#) and the ethical guidelines, outlined in our [author and reviewer resource centre](#), still apply. In no event shall the Royal Society of Chemistry be held responsible for any errors or omissions in this Accepted Manuscript or any consequences arising from the use of any information it contains.





Journal Name

ARTICLE

Discovery and Optimization of Selective Inhibitors of Protein Arginine Methyltransferase 5 by Docking-Based Virtual Screening

Yan Ye,^{†a,b} Bidong Zhang,^{†a,b} Ruifeng Mao,^a Chenhua Zhang,^c Yulan Wang,^a Jing Xing,^a Yu-Chih Liu,^c Xiaomin Luo,^a Hong Ding,^a Yaxi Yang,^d Bing Zhou,^d Hualiang Jiang,^{a,d} Kaixian Chen,^{a,d} Cheng Luo,^{*a} and Mingyue Zheng,^{*a}

Received 00th January 20xx,
Accepted 00th January 20xx

DOI: 10.1039/x0xx00000x

www.rsc.org/

Protein arginine methyltransferase-5 (PRMT5) is a type II PRMT enzyme critical for diverse cellular processes and different types of cancers. Many efforts have been dedicated toward discovering novel scaffold PRMT5 inhibitors. Herein, we report the discovery of DC_P33 as a hit compound of PRMT5 inhibitor, identified by a molecular docking based virtual screening and ³H-labeled radioactive methylation assay. Structure–activity relationship (SAR) analysis was performed on the analogs of DC_P33, and then structure modifications were made to improve its activity. Among the derivatives, the compound DC_C01 displayed an IC₅₀ value of 2.8 μM, and good selectivity over PRMT1, EZH2 and DNMT3A. Moreover, DC_C01 exhibited anti-proliferation activities against Z-138, Maver-1, and Jeko-1 cancer cells with EC₅₀ value of 12 μM, 12 μM, and 10.5 μM, respectively. Taken together, these results contribute to the development of specific inhibitors against PRMT5 and cancer therapy.

Introduction

Protein arginine methyltransferases (PRMTs) are a family of enzymes that catalyze the transfer of a methyl group from S-adenosylmethionine (SAM) to the guanidine nitrogen of an arginine residue,¹ involved in the regulation of cellular processes, such as RNA processing, transcription, DNA repair and signal transduction.^{2–7} Currently, nine human PRMTs (PRMT1–9) have been reported in mammals.^{8,9} These PRMTs are classified into three types of arginine methylation based on the catalytic mechanism. PRMT5 is a type II PRMT enzyme, which is currently to be the dominant enzyme for symmetric dimethylarginines (SDMA).^{10, 11} PRMT5 methylates the substrate of histone H3 (H3R8me2s) and H4 (H4R3me2s), which promotes transcriptional repression by changing chromatin structure.^{12–14} PRMT5 has been found to be overexpressed in different types of cancers, including leukemia,

lymphoma, lung cancer, colorectal cancer and breast cancer.^{13, 15–17} In addition, PRMT5 plays a role in the proliferation and survival of mantle cell lymphoma (MCL) and diffuse large B-cell lymphoma (DLBCL) cells.¹³ RNAi knockdown of PRMT5 in embryonic stem (ES) cells results in down-regulation of pluripotency-associated genes and up-regulation of differentiation-associated genes,⁷ and shRNA knockdown of PRMT5 in lymphoblastoid cell lines results in decreased viability.¹⁸ These observations suggest that PRMT5 is a promising therapeutic target for cancers. Till now, many efforts have been taken in discovering small-molecule inhibitors against PRMT5. Sinefungin is a highly potent and SAM-competitive PRMT5 inhibitor. However, due to its structural similarity to SAM, sinefungin shows no selectivity against various methyltransferases such as other PRMTs and protein lysine methyltransferases. In the past years, high-throughput screening (HTS) has been adopted to discover PRMTs inhibitors.^{17, 19–22} Spannhoff et al. identified stilbamidine as a competitive inhibitor of the substrate using a target-based virtual screening approach, which showed an IC₅₀ value of 44.1 μM against PRMT5.²³ These compounds are pan-methyltransferase inhibitors and display nonspecific interaction to PRMT5.¹ Alinari et al. discovered a first-in-class, highly selective, small-molecule PRMT5 inhibitor CMP5.¹⁸ This compound is predicted to occupy in the SAM-binding pocket, showing an IC₅₀ value lower than 50 μM. Recently, a selective and potent PRMT5 inhibitor EPZ015666 with an IC₅₀ value of 0.022 μM was reported, and it displayed anti-tumor activity in MCL xenograft animal models.²⁴ A phase 1 clinical study has been initiated by GSK to investigate the safety, pharmacokinetics, pharmacodynamics of an analog of

^a Drug Discovery and Design Center, State Key Laboratory of Drug Research, Shanghai Institute of Materia Medica, Chinese Academy of Sciences, 555 Zuchongzhi Road, Shanghai 201203, China.

^b University of Chinese Academy of Sciences, No.19A Yuquan Road, Beijing 100049, China.

^c Shanghai ChemPartner Co., Ltd., #5 Building, 998 Halei Road, Shanghai 201203, China.

^d School of Life Science and Technology, Shanghai Tech University, Shanghai 200031, China.

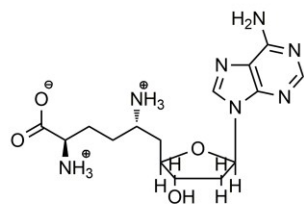
^e Department of Medicinal Chemistry, Shanghai Institute of Materia Medica, Chinese Academy of Sciences, Shanghai 201203, China.

[†]Electronic Supplementary Information (ESI) available: Structure of the human PRMT5 with cofactor SAM and EPZ015666. The Specs IDs of brought compounds. HPLC analysis data of synthesized compounds. ¹H and ¹³C NMR spectra. See DOI: 10.1039/x0xx00000x

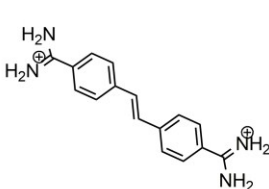
[‡]These authors contributed equally to this work.

ARTICLE

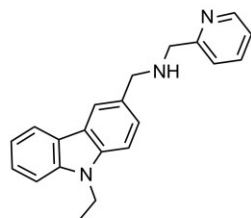
Sinefungin

PRMT5 (Ki) = 0.51 μ M

Stibamidine

PRMT5 (IC₅₀) = 44.1 μ M

CMP5

PRMT5 (IC₅₀) < 50 μ M

EPZ015666

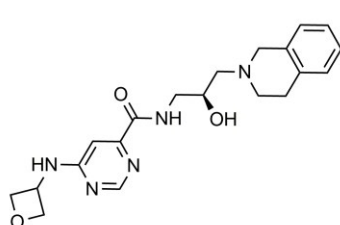
PRMT5 (IC₅₀) = 0.022 μ M

Fig.1 The reported inhibitors against PRMT5.

EPZ015666.²⁵ The structures of the published PRMT5 inhibitors and their activities are summarized in Fig.1. Unfortunately, there are limited inhibitors with high potency and selectivity. The discovery of potent and selective PRMT5 inhibitors with novel scaffolds is thus of high interest to the field of PRMT5 biology and related medicinal chemistry studies.

With the rapid development of computational methods, many studies have successfully discovered new epigenetic

inhibitors using virtual screening.²⁶⁻²⁹ In our group, virtual screening methods have been used to identify inhibitors of PRMT1, DNMT1, SET7, etc.²⁸⁻³⁰ These successful experiences encourage us to utilize virtual screening method to discover novel inhibitors of PRMT5. In this research, a promising hit was first discovered by virtual screening. Similarity-based searching and medicinal chemistry approaches were then applied in the optimization of the hit, and to study the structure-activity relationship (SAR) of these inhibitors.

Results and discussion

Docking-Based Virtual screening.

The PRMT5 has two ligand binding pockets: a SAM-binding site and a substrate-binding pocket, as shown in Fig.S1. In order to find inhibitors with better selectivity profile, we chose to use the substrate-binding pocket for virtual screening because the SAM-binding site is shared by various histone and DNA methyltransferases. Recently, the cofactor SAM was reported forming essential interactions with the methyl group-accepting inhibitor EPZ015666 and hence contributing to the binding affinity of the substrate-competitive inhibitors to PRMT5.²⁴ Accordingly, SAM was kept as a part of the receptor structure in our docking-based screening. Currently, there are seven different crystal structures of PRMT5 available in Protein Data Bank. The crystal structure (PDB id 4X61) was used for molecular docking because it contains both the methyl donor SAM and a substrate-competitive inhibitor EPZ015666. To test the "screening power" of the structure model, we collected 20 active derivatives of the inhibitor EPZ015666 from the published patents.³¹ Totally 720 decoys were compiled at a

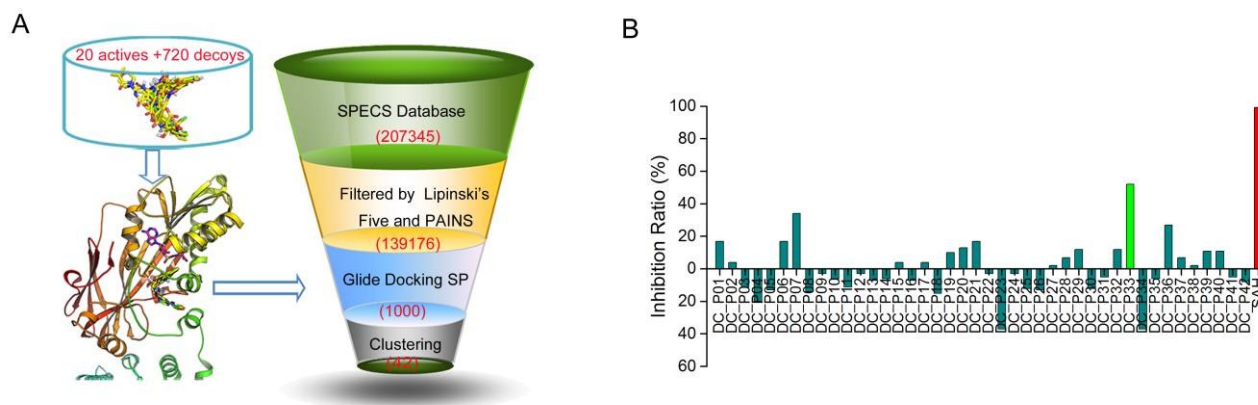


Fig.2 Virtual screening workflow and *in vitro* inhibitory activity assay results for the selected compounds. (A) Schematic representation of the whole screening procedures. (B) Inhibitory activity for all compounds at the concentration of 50 μ M. The red column represents the activity of the reference compound SAH.

ARTICLE

ratio of 1:36 with DecoyFinder V1.1.³² All the actives and decoys were docked into the model separately. Consequently, the area under receiver operating characteristic curve (AUC) of the model is 0.93, while the 2% enrichment factor (EF) of the model is 35. Therefore, the structure model was used in our subsequent screening procedures.

The workflow of virtual screening is shown in Fig.2A. A commercially available compound library SPECS (<http://www.specs.net>), which includes 207342 compounds was used as the ligand database. Filtered by "Lipinski's Rule of Five" and the structural patterns of pan-assay interference structures (PAINS),³³ the remaining 139176 compounds were prepared and docked into the substrate site of the prepared protein. Details about the ligand preparation and molecular docking are provided in Method section. The top ranked 1000 molecules were selected and clustered, accounting for both structural diversity and the interactions with key residues such as Phe327, Phe580 or Glu444. Finally, 42 molecules were selected and purchased for the subsequent biochemical assay evaluation.

PRMT5 Inhibition Assays.

The virtual screening selected compounds were tested for activity against PRMT5 using ³H-labeled radioactive methylation assay. Fig.2B depicted the inhibition ratio of 42 compounds against PRMT5 at the concentration of 50 μ M, with S-adenosyl-L-homocysteine (SAH) used as a reference. From the enzyme inhibition assay, DC_P33 showed the most potent inhibitory activity against PRMT5 with the inhibition ratio of 52%. In a more quantitative analysis, we measured the activity of DC_P33 against PRMT5 at a range of concentrations and the IC₅₀ is 35.6 μ M. Therefore, DC_P33 was selected as a hit compound for further optimization.

Similarity-Based Analog Searching.

In order to verify the scaffold of DC_P33 and to investigate the structure-activity relationship of its analogues, we performed the second round of screening based on a chemical fingerprint similarity searching. Finally, 14 analogues of DC_P33 were selected and purchased for activity evaluation. Five compounds show more than 50% inhibitory activity against PRMT5 at the concentration of 50 μ M, which were further evaluated for the inhibitory activity within a range of concentrations. The biochemical assay results and structures of these compounds are shown in Table 1.

Binding Mode Prediction of DC_P33.

As shown in Fig.3A, the compound DC_P33 consists of three parts: a naphthalene ring and two substituents denoted as **A** chain (-CH₂NHCH₂CH₂OH) and **B** chain (-benzyloxy), respectively. To analyze its interaction with PRMT5, the putative binding mode of DC_P33 was compared with the crystal structure of EPZ015666, which is shown in Fig.3B and Fig.3C. Similar to the binding mode of the tetrahydroisoquinoline (THIQ) in EPZ015666, **A** chain of DC_P33 is situated in the hydrophobic pocket composed by Leu319, Tyr324, Phe327 and Trp579. This explained that increased hydrophobic interaction in R₂ position of scaffold **I** (DC_S08, DC_S09, DC_S10 and DC_S11) improved potency, while long polar chains in the same position (DC_S04, DC_S05 and DC_S06) significantly reduced the activity of the compounds. Another feature of EPZ015666 is that the terminal pyrimidine forms π - π stacking interactions with Phe327 and Phe580. Similar π - π interactions are observed for the phenyl group of the **B** chain in DC_P33, and removing the phenyl group (DC_S12, DC_S13 and DC_S14) resulted in markedly decreased activity. There are also differences between DC_P33 and EPZ015666. For example, the phenyl of the THIQ in EPZ015666 forms cation- π interaction with the partial charged

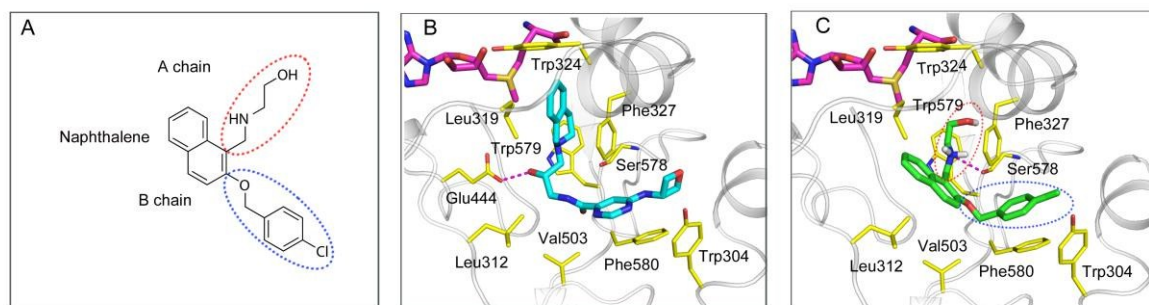


Fig.3 The putative binding mode of DC_P33 in the substrate-binding site of PRMT5: (A) DC_P33 contains three parts: a naphthalene ring, **A** chain (dash red box) and **B** chain (dash blue box); (B) The binding mode of EPZ015666 (cyan); (C) The binding mode of DC_P33 (green). SAM is displayed as magenta color.

ARTICLE

methyl group of SAM, and also forms π - π stacking interaction with Phe327, a conserved residue critical for directing the ability of PRMT5 to catalyze SDMA.³⁴ These interactions are all missing in DC_P33, as highlighted in the red circle in Fig.3C. Apparently, it can be inferred that introducing an aromatic ring into the **A** chain may help to improve the activity of DC_P33.

Hit optimization and SAR analysis.

To test the above inference, we designed and synthesized 19 compounds. The biochemical assay results and structures of these compounds are shown in Table 2. Among these compounds, DC_C01 is the most potent with an IC_{50} value of 2.8 μ M (Fig.4B), and it exhibits up to 12-fold more increase in dose potency against PRMT5 over DC_P33. As shown in Fig.4A,

DC_C01 was obtained from DC_P33 by adding a phenyl group next to the hydroxyl group in the **A** chain and removing a chloride group from the phenyl in the **B** chain. According to the putative binding mode of DC_C01 shown in Fig.4C, the added phenyl group is situated at the same position of THIQ, forming cation- π interaction with the positively charged SAM.

The **A** chain is situated in a hydrophobic pocket near to the SAM-binding pocket. As shown in Fig.4C, the hydroxyl group in the **A** chain has no obvious effect for the binding of compound DC_C01 to PRMT5. Removing the hydroxyl group, DC_C08 possesses an IC_{50} value of 3.2 μ M, which has comparable potency to DC_C01. This result implies that the hydroxyl group of the **A** chain is not essential to their binding to PRMT5.

Table 1 Biochemical Assays results for DC_P33 and its analogues selected by similarity-based searching.

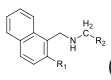
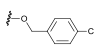
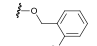
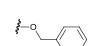
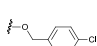
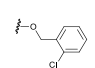
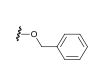
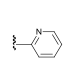
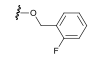
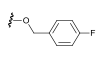
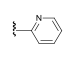
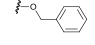
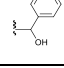
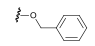
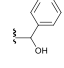
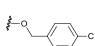
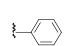
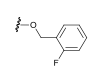
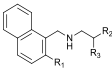
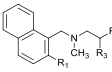
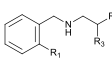
 (I)							
Entry	R ₁	R ₂	Inhibition Rate at 50 μ M (IC_{50}/μ M)	Entry	R ₁	R ₂	Inhibition Rate at 50 μ M (IC_{50}/μ M)
DC_P33		-CH ₂ OH	52% (35.6)	DC_S08		-CH(CH ₃)OH	69% (15)
DC_S01		H	32%	DC_S09		-CH ₂ N(CH ₃) ₂	79% (8.5)
DC_S02		-CH ₂ OH	48%	DC_S10			68% (22)
DC_S03		-CH ₂ OH	22%	DC_S11			57% (15)
DC_S04		-CH ₂ CH ₂ NHCH ₃	10%	DC_S12	-OCH ₂ CH ₃		46%
DC_S05		-CH ₂ NHCH ₂ CH ₂ OH	19%	DC_S13	H		2%
DC_S06		-CH ₂ NHCH ₂ CH ₂ OH	24%	DC_S14	-OCH ₃		38%
DC_S07		-CH ₂ OCH ₃	76% (12)				

Table 2. Biochemical Assays results for 19 synthesized analogues of DC_P33.

View Article Online

DOI: 10.1039/C7OB00070G

<div style="display: flex; justify-content: space-around; align-items: center;"> <div style="text-align: center;">  <p>(II)</p> </div> <div style="text-align: center;">  <p>(III)</p> </div> <div style="text-align: center;">  <p>(IV)</p> </div> </div>						
Entry	Scaffold	R ₁	R ₂	R ₃	IC ₅₀ /μM	Inhibition Rate at 50 μM
DC_P33	II		H	-OH	35.6	-
DC_C01				-OH	2.8	-
DC_C02				-OH	8.4	-
DC_C03				-OH	-	5%
DC_C04				-OH	-	25%
DC_C05				-OH	9.1	-
DC_C06				-OH	9.6	-
DC_C07				-OH	29	-
DC_C08				H	3.2	-
DC_C09				H	7.9	-
DC_C10				H	4.5	-
DC_C11				H	38	-
DC_C12				H	45	-
DC_C13				H	4.1	-
DC_C14				H	6.4	-
DC_C15				H	13	-
DC_C16				H	25	-
DC_C17				H	4.3	-
DC_C18	III			H	-	9%
DC_C19	IV			-OH	25	-

ARTICLE

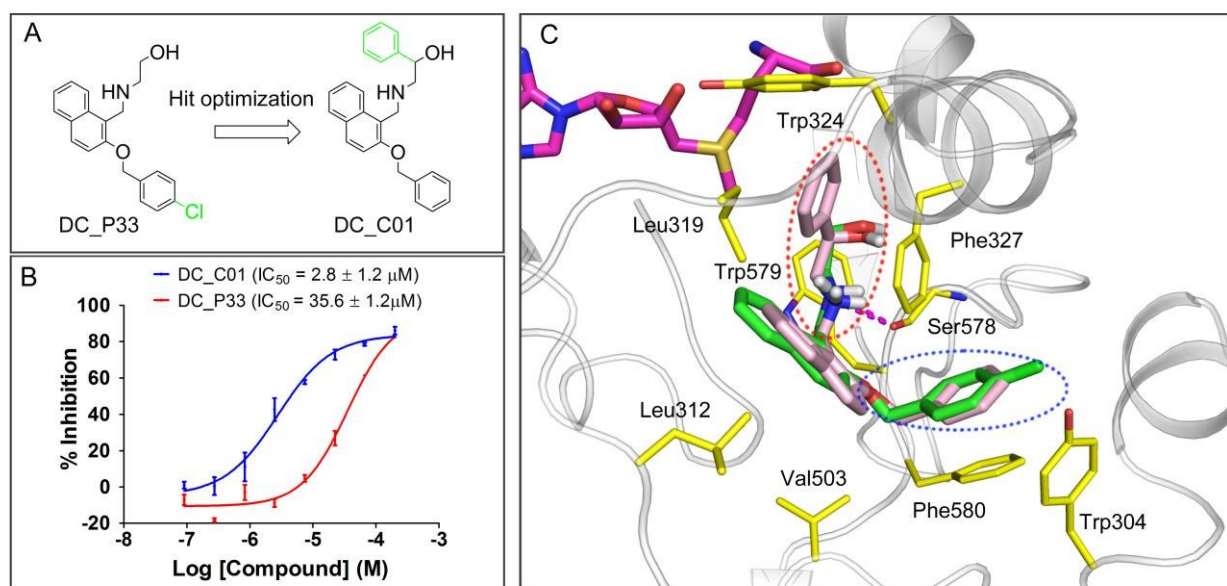


Fig. 4 The optimization of DC_P33 to DC_C01. (A) The strategy for hit optimization; (B) The IC_{50} values for DC_P33 and DC_C01; (C) The superimposition of the putative binding modes of DC_P33 and DC_C01.

As mentioned above, the phenyl group of the **A** chain is predicted to form cation- π interaction with SAM. To further confirm it, four analogues with the phenyl group replaced by different aromatic and non-aromatic rings were synthesized. As shown in Table 2, the activities of these compounds are -phenyl > - (3-Indolyl) > - (2-pyridyl) > - (1-piperidyl) > 4-morpholinyl. The hetero-nonaromatic ring DC_C11 (R_2 = 1-piperidyl) and DC_C12 (R_2 = 4-morpholinyl) exhibited 11.9-fold and 14.1-fold lower activities than DC_C08 (R_2 = phenyl). These results agree well with our previous inference that the cation- π interaction of this moiety is very important to the activity of the compounds. A series of substituents such as fluorine, hydroxyl, methyl and chloride were incorporated into the para-position of the phenyl. All the compounds displayed lower potencies than DC_C08. Particularly, the chloride substituent DC_C16 showed 7.8-fold loss of potency. Since the phenyl ring of the **A** chain is situated at a small hydrophobic cavity surrounding by Leu319, Tyr324, and Phe327 (Fig. 4C), the steric hindrance may lead to their decreased activities.

For DC_P33, the interaction with SAM is missing, but the secondary amine group in **A** chain can be protonated and form cation- π interactions with Phe327 and Trp579. Moreover, there is a hydrogen bond between the amine group and the backbone carbonyl of Ser578, which also highlighted the importance of the amine group in ligand binding. The methylation of the amine group obtaining DC_C18 destroys

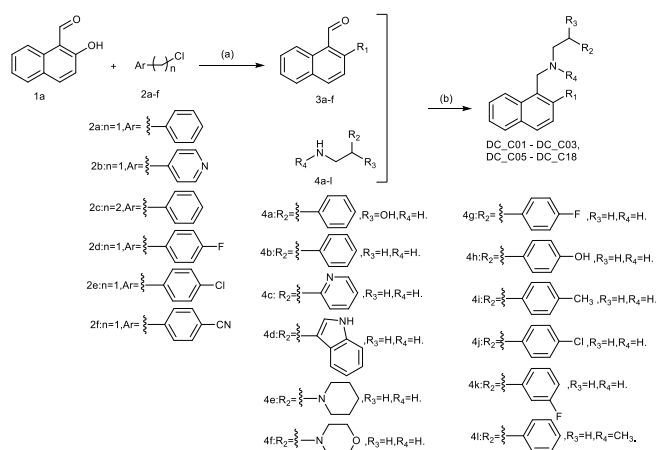
the hydrogen-bonding interaction, and therefore results in a complete loss of activity, with the inhibition ratio of 9% at the concentration of 50 μ M. This result confirms that the hydrogen bond between the amine group and residue Ser578 is essential to the inhibitory activity against PRMT5.

As shown in Fig. 4C, the naphthalene ring is snug into the hydrophobic pocket surrounded by residue Leu312, Leu319, Phe327 and Val503. The replacement of the naphthalene ring with a smaller phenyl ring decreased the hydrophobic interaction, which may explain that DC_C19 showed about 8.9-fold less potent PRMT5 inhibitory activity (IC_{50} = 25 μ M) than DC_C01 (IC_{50} = 2.8 μ M). The phenyl ring on the **B** chain forms π - π stacking interaction with residue Phe327 and Phe580. Removing **B** chain (DC_S13) or changing its length (DC_C03) completely abolished the activity, and replacing the phenyl ring on the **B** chain by a methyl group (DC_S12) or an electron-deficient pyridine (DC_C02) also showed significantly decreased potency.

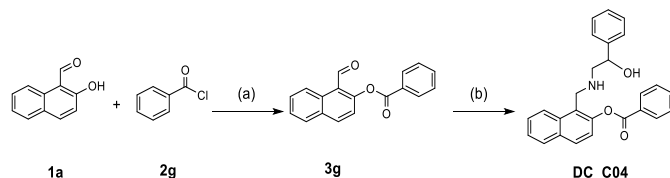
Synthesis.

We have optimized the chemical structure in order to improve the inhibitory activity. Initially, the treatment of the readily available 2-hydroxy-1-naphthaldehyde **1a** with (chloromethyl)-benzene **2a** using anhydrous K_2CO_3 as a base at reflux to furnish key intermediate 2-(benzyloxy)-1-naphthaldehyde **3a**.^{35,36} Then, the product DC_C01 was prepared by reductive

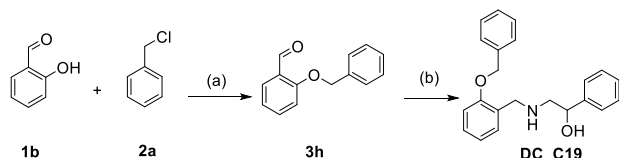
ARTICLE

Scheme 1 General synthesis of compounds (DC_C01 to DC_C03 and DC_C05 to DC_C18)

Reagents and conditions: (a) PhCH_2Cl (1.2 equiv), KI (0.2 eq), anhydrous K_2CO_3 (1.2 equiv), dry acetone, reflux, 4–6 h, 65–95%; (b) alkylamine 4a–l (1.2 equiv), $\text{NaBH}(\text{OAc})_3$ (3.0 equiv), CH_3COOH (1.0 equiv), DCE, room temperature, 2–4 h, 83–97%.

Scheme 2 Synthesis of compound DC_C04

Reagents and conditions: (a) PhCOCl (1.5 equiv), anhydrous K_2CO_3 (1.5 equiv), dry THF, room temperature, 16 h, 75%; (b) 2-amino-1-phenylethan-1-ol 4a (1.2 equiv), $\text{NaBH}(\text{OAc})_3$ (3.0 equiv), CH_3COOH (1.0 equiv), DCE, room temperature, 3 h, 77%.

Scheme 3 Synthesis of compound DC_C19

Reagents and conditions: (a) PhCH_2Cl 2a (1.2 equiv), KI (0.2 equiv), anhydrous K_2CO_3 (3.0 equiv), dry acetone, reflux, 4.5 h, 88%; (b) 2-amino-1-phenylethan-1-ol 4a (1.2 equiv), $\text{NaBH}(\text{OAc})_3$ (3.0 equiv), CH_3COOH (1.0 equiv), DCE, room temperature, 3.5 h, 87%.

aldehydes **3a** with the commercial 2-amino-1-phenylethan-1-ol **4a** in the presence of acetic acid and $\text{NaBH}(\text{OAc})_3$ with good to high yield.^{37, 38} Similar approach was employed for synthesis of compounds DC_C02, DC_C03 and DC_C05 – DC_C18, utilizing

different aromatic-substituted alkyl chlorides (**2b–2f**) and alkylamine compounds (**4b–4l**) with diverse substituents, which is depicted in Scheme 1.

Compound DC_C04 was synthesized using the route described in Scheme 2. As acyl chloride is very active and easily produces much more side products, mild condition (room temperature) was accomplished to afford the key intermediate compound **3g** in moderate yield.³⁹ Subsequent reductive amination as previously described using amine **4a** afforded the desired compound DC_C04 in 77% yield.

Additionally, in order to investigate the role of the naphthalene ring, benzene ring was readily introduced to provide the product DC_C19, as outlined in Scheme 3. Starting with the monocycle 2-hydroxybenzaldehyde **1b**, the compound 2-(benzyloxy)benzaldehyde **3h** was prepared according to previous procedures and subsequent reductive amination.

Methyltransferase Enzymatic Selectivity of DC_C01.

Methylation of DNA and histone proteins are mutually involved in the epigenetic regulation of gene expression mediated by DNA methyltransferases (DNMTs) and histone methyltransferases (HMTs). DNMTs methylate cytosine residues within gene promoters, whereas HMTs catalyze the transfer of methyl groups to lysine and arginine residues of histone proteins. To investigate the selectivity of DC_C01 for the pre-dominant type II arginine methyltransferase PRMT5, we also evaluated its activity on other three different types of methyltransferases, including protein arginine methyltransferase 1 (PRMT1), the representative of type I arginine methyltransferase, DNA methyltransferase 3A (DNMT3A) and enhancer of zeste homolog 2 (EZH2), one of lysine methyltransferases. First, we conducted a multiple sequence alignment of the substrate-binding site of PRMT5, PRMT1, DNMT3A and EZH2. As shown in Fig.5A, the substrate-binding sites of these methyltransferases are not highly conserved, especially for EZH2. The sequences of PRMT1 and DNMT3A share relatively higher homology with PRMT5. Then, a structural alignment of PRMT5, PRMT1 and DNMT3A was performed. As shown in Fig.5B, the substrate-pocket structure of DNMT3A can not be aligned well with that of PRMT5, and it is hence inaccessible to the binding of DC_C01. For PRMT1, there are also clear differences with PRMT5, e.g., the residues Phe327 and Phe580 of PMRT5 that form important π - π interaction the inhibitory activity of DC_C01 against PRMT1, with DC_C01 are replaced as Met and Lys, respectively, and the interaction was therefore abolished. Moreover, the substitution of Ser439 in PRMT5 with Tyr148 in PRMT1 reveals that the tryptophan may reduce the size of the substrate-binding pocket, and sterically hinder the binding of substrate

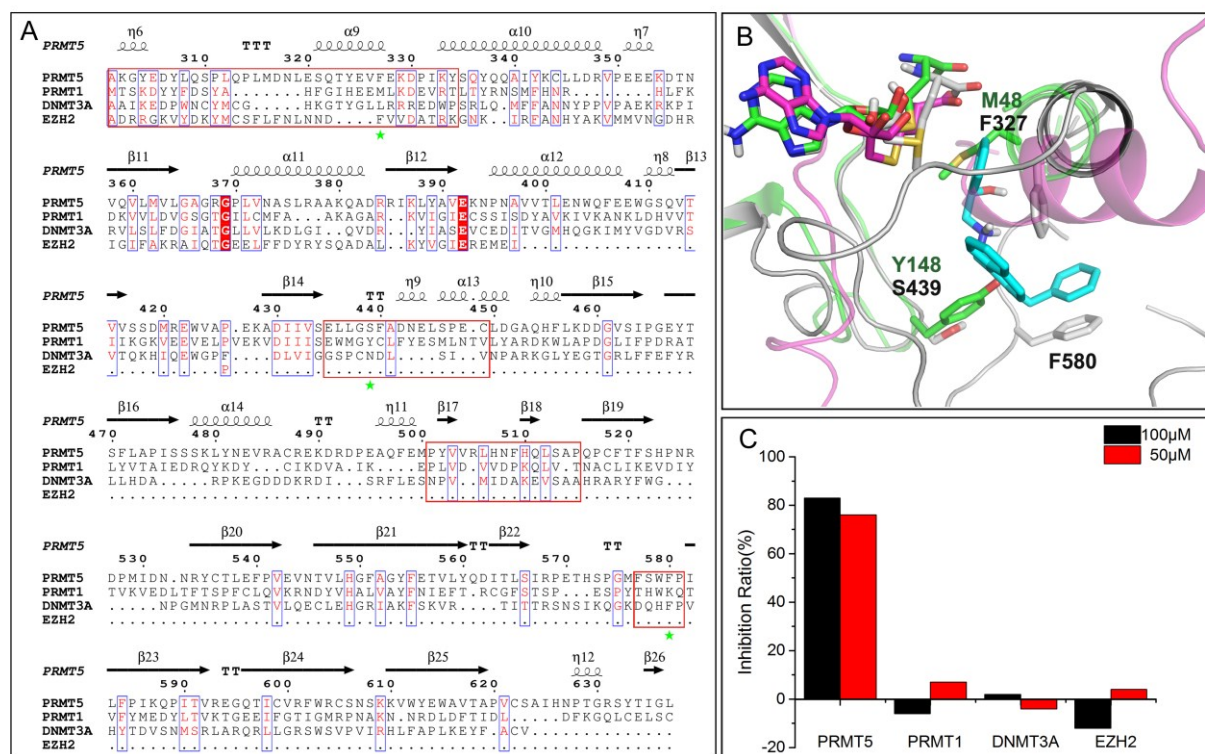


Fig.5 Selectivity of DC_C01 over different DNA and histone methyltransferases. (A) Sequence alignment of the substrate-binding sites of PRMT5, PRMT1, EZH2 and DNMT3A. Some important amino acids in the substrate-binding site of PRMT5 are marked in red boxes. (B) Superimposition of the substrate-binding domains of PRMT5 (PDB id: 4X61, gray color), PRMT1 (PDB id: 1or8, green color) and DNMT3A (PDB id: 3hyn, magenta color). DC_C01 is shown in cyan stick. (C) Inhibition ratio of DC_C01 over PRMT5, PRMT1, EZH2 and DNMT3A at the concentration of 50 μM and 100 μM.

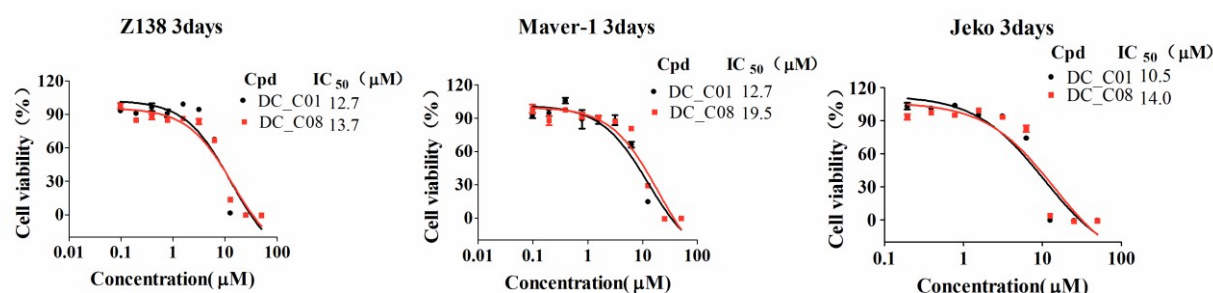


Fig.6 DC_C01 and DC_C08 effects on in vitro Cellular proliferation in MCL cell lines.

and DC_C01. This effect is partially supported by a previous report that mutating Ser439 to a tryptophan significantly decreased the enzymatic activity of PRMT5.³⁴ Through the sequence and structural alignment analyses, we may find that the substrate-binding sites of different methyltransferases reveal apparent diversities, which enable the design of

selective PRMT5 inhibitor. Finally, we assessed and compared PRMT5, EZH2 and DNMT3A, using the radioactive methylation assay at the concentration of 50 μM and 100 μM (Fig.5C). Not unexpectedly, DC_C01 showed potent activity against PRMT5, while it is inactive to PRMT1, EZH2 and DNMT3A. Therefore,

these results suggested that the compound DC_C01 exhibited good selectivity toward PRMT5.

Cell-based Activity.

PRMT5 is reported to have a role in MCL, as evidenced not only by upregulation of PRMT5 in patient samples, but also by anti-proliferative effects observed after PRMT5 knockdown in MCL cell lines.^{12, 13, 40, 41} A panel of three MCL cell lines (Z-138, Maver-1 and Jeko-1) were used to assess proliferation effects upon treatment with PRMT5 inhibitors allowing for the measurement of cell growth over 3 days. As shown in Fig.6, DC_C01 and DC_C08 inhibit the proliferation in a dose-dependent manner. DC_C01 exhibited potent anti-proliferative activities against Z-138, Maver-1, and Jeko-1 cancer cells with EC₅₀ values of 12.7 μ M, 12.7 μ M, and 10.5 μ M, respectively. DC_C08 demonstrated that biochemical inhibition is well correlated with proliferation, with EC₅₀ values ranging from 13.7 μ M to 19.5 μ M. These results suggest that both of DC_C01 and DC_C08 inhibit the proliferation of Z-138, Maver-1, and Jeko-1 cancer cells.

Conclusions

Protein arginine methyltransferases play significant roles in the regulation of cellular processes, such as RNA processing, transcription, DNA repair and signal transduction. Inhibition of PRMT5 is a novel therapeutic approach for the treatment of cancer. Currently, there are limited inhibitors in reported studies which are specific to PRMT5. In the present study, we discovered the compound DC_P33 as a novel inhibitor of PRMT5 with an IC₅₀ value of 35.6 μ M using the docking-based virtual screening. Subsequently, 14 derivatives of DC_P33 were obtained from SPECS database by the similarity-based searching method. Five of them were found to show more than 50% inhibition of PRMT5 at the concentration of 50 μ M. Combining the binding mode of DC_P33 with the activity of its analogues, we further designed and synthesized 19 analogues of DC_P33. Among these compounds, DC_C01 showed the highest potency against PRMT5 with an IC₅₀ value of 2.8 μ M. The selectivity profile of DC_C01 on various DNA and histone methyltransferases including of PRMT5, PRMT1, DNMT3A and EZH2 were also investigated. By structural analyses and biochemical assay evaluation, DC_C01 was identified to show clear specificity for PRMT5. Finally, DC_C01 and DC_C08 were evaluated for their anti-proliferative effects in the Z-138, Maver-1, and Jeko-1 cancer cells, and they inhibited the proliferation of all the three cancer cells in a dose-dependent manner. The study presented here details the discovery of potent, selective PRMT5 inhibitors with a novel scaffold using a structure-guided drug design approach, which provide useful starting point and information for the further development of epigenetic drugs for cancer therapy and the related chemical biology studies.

Experimental

Virtual screening

Preparing the protein structure. The crystal structure of PRMT5 with cofactor SAM and small inhibitor EPZ015666 was retrieved from Protein Data Bank (PDB id: 4X61). The protein structure was prepared in the Protein Preparation Wizard Workflow of the Schrödinger software package (Schrödinger, LLC, New York, NY, 2010). SAM was remained because it formed cation- π interaction with the inhibitor. All waters were deleted from the PRMT5 structures, and hydrogens were added. The orientations and tautomeric states of Gln, Asn and His were optimized to better from the hydrogen bonds. The complex was then minimized with the OPLS_2005 force field and a maximum rmsd of 0.30 Å to restrain steric clashes. Next, a three-dimensional grid was generated with the Receptor Grid Generation module in the Maestro program (Maestro, version 9.1; Schrödinger, LLC: New York, NY, 2010), on the size and centroid of the ligand EPZ015666.

Preparing the Ligand Database. In total, 207342 compounds were obtained from SPECS database. Compounds containing pan-assay interference structures (PAINS) were removed and the remaining 187842 compound were then filtered by "Lipinski's Rule of Five" to remove compounds which may have poor absorption or permeability in Pipeline Pilot (Pipeline Pilot, version 7.5; Accelrys Software Inc.: San Diego, CA). Finally, 139176 compounds were prepared in LigPrep module (LigPrep, version 2.4; Schrödinger, LLC: New York, NY, 2010). First these structure were optimized with OPLS_2005 force field. The ionization state of the structures were subsequently generated using Epik (Epik, version 2.1; Schrödinger, LLC: NewYork, NY, 2010) method at target pH 7 \pm 2.0. The specified chirality of the ligands was retained and other chiral centers were varied. The stereoisomers were generated at most 32 per ligand. The generating structures were used for virtual screening.

Glide Docking Procedure. The prepared receptor and ligand files were imported in the Ligand Docking module using Glide software (Glide, version.6; Schrödinger, LLC: New York, NY, 2010) with the standard precision mode (SP). The top-ranked 1000 poses were chosen to group into 100 clusters with Pipeline Pilot. After visual inspection of the binding poses of the compounds, 42 molecules with structural diversity and binding affinity were selected and purchased for biological assay test. **Table S1** lists the docking scores and ranks of 42 compounds before any manual selection.

Similarity-based analogues searching. It was shown from the biological test that compound DC_P33 was most potent. In order to obtain derivatives of DC_P33, the SPECS database filtered by PAINS was searched in Pipeline Pilot with Tanimoto coefficient and ECFP_4 fingerprints. The cutoff was set to 0.50. A total of 14 analogues were found by the threshold of the similarity and bought for biological test.

Commercial Compounds. Fifty-six compounds (DC_P01-42, DC_S01-14) were purchased from SPECS. The purity of all these compounds are reported in **Table S1** and **Table S2**. The purity of the active compounds is equal to or greater than 95%.

PRMT5 Inhibition Assays.

The radioactive PRMT5 methylation inhibition assay was performed in 25 μ L reaction system containing adenosyl-L-methionine S-[methyl-³H] (³H-SAM, 15.4 Ci/mmol, PerkinElmer), biotinylated H4 derived peptide (synthesized by GL China) and 1 nM PRMT5/MEP50 (BPS, 51045) in modified Tris Buffer, pH 8.0. The protein was pre-incubated with a range of compound concentrations for 15 min at room temperature before adding

biotinylated peptide and [³H]SAM. After 60 min of incubation at room temperature, the reaction was stopped and was transferred to a 384-well streptavidin-coated Flashplate (PerkinElmer) and was incubated for another 1h at room temperature. The Flashplate was washed with dH₂O + 0.1% Tween-20 for three times and the radioactivity was determined by liquid scintillation counting (MicroBeta, PerkinElmer). IC₅₀ values were derived by fitting the data for the inhibition percentage to a dose-response curve by nonlinear regression in GraphPad Prism 5.0.

Methyltransferase Enzymatic Selectivity Assay.

PRMT1, EZH2 and DNMT3A radioactive methylation inhibition assays were similar to that of PRMT5. The radioactive PRMT1 methylation inhibition assay was performed in 25 μ L reaction system containing ³H-SAM, biotinylated H4 derived peptide (synthesized by GL China) and 0.5 nM PRMT1 (BPS, 51041) in modified Tris Buffer, pH 8.0. The radioactive EZH2 methylation inhibition assay was performed in 25 μ L reaction system containing ³H-SAM, biotinylated H3 derived peptide (synthesized by GL China) and 3 nM EZH2 (BPS, 51004) in modified Tris Buffer, pH 9.0. The radioactive DNMT3A methylation inhibition assay was performed in 30 μ L reaction system containing ³H-SAM, biotinylated DNA oligonucleotides (synthesized by Life Technologies) and 12.5 nM DNMT3A (BPS, 51106) in modified Tris Buffer, pH 8.0. The proteins were preincubated with 50 μ M and 100 μ M of compound DC_C01 for 15 min at room temperature before substrates and [³H]SAM were added. After 60 min of incubation at room temperature for PRMT1 and EZH2 assays, or after 4h of incubation at room temperature for DNMT3A assay, the reactions were stopped and were transferred to a 384-well streptavidin-coated Flashplate and then incubated for 1h at room temperature. The Flashplate was washed with dH₂O + 0.1% Tween-20 for three times and the radioactivity was also determined by liquid scintillation counting. Fit the data in Excel to obtain inhibition percentage using equation: $\text{Inh \%} = (\text{Max-Signal}) / (\text{Max-Min}) * 100$.

In vitro proliferation assay.

For assessment of the effect of DC_C01 and DC_C08 treatment on the cell lines, they were plated in 96-well plates at a density of 1 \times 10⁵ cell/well in 100 μ L media. After 6 hours of incubation, the increasing concentrations of DC_C01 and DC_C08 (0-100 μ M) were added to the medium for an additional 3 days. Viable cell number was determined using the Cell Titer-Glo Luminescent Cell Viability assays (Promega), and luminescence was recorded using an EnVision Multilabel Plate Readers (PerkinElmer) according to the manufacturer's protocol. For each cell line, the concentration-dependence curves were determined at each time point using Graphpad Prism software.

Chemistry.

Commercially available chemicals were used without further purification. All products were characterized by their NMR and MS spectra. ¹H NMR spectra were recorded with a Varian-MERCURY Plus-400 NMR spectrometer. ¹³C NMR spectra were recorded with a Varian-MERCURY Plus-500 NMR spectrometer. Chemical shifts are reported in ppm (δ scale) as referenced to TMS and coupling constant (J) values are reported in hertz (Hz).

Data are presented as follows: chemical shift, multiplicity (s = singlet, d = doublet, dd = doublet of doublet, t = triplet, q = quartet, m = multiplet, br = broad), coupling constant in Hz, and integration. Low-resolution and high-resolution mass spectrometry (LRMS/HRMS) were recorded on a Thermo - DFS spectrometer. Flash and column chromatography was performed using silica gel (200–300 mesh). Analytical TLC was performed silica gel plates and visualized under ultraviolet light (254 nm). The purity of the target compounds was determined to be >95% by analytical HPLC.

Procedures for synthesis of compounds. Synthesis of the presented compounds were performed according to Schemes 1–3. Synthesis and analytical data for representative compounds are provided below.

The synthesis of 2-(benzyloxy)-1-naphthaldehyde. To a solution of commercially available 2-hydroxy-1-naphthaldehyde **1a** (2.58 g, 15.00 mmol) in dry acetone (50 mL) was added anhydrous K₂CO₃ (2.50 g, 18.00 mmol) and (chloromethyl)benzene **2a** (2.28 g, 18.00 mmol) and KI (500 mg, 3.00 mmol) refluxed for 4h. The mixture was then filtered through Celite and the filter cake was well washed with acetone (50 mL). The filtrate was concentrated and the resulting residue was redissolved in ethyl acetate (100 mL), washed with water (2 \times 100 mL) and brine (50 mL). The organic layer was dried over anhydrous Na₂SO₄, filtered, and then concentrated in vacuo. Purification of the crude product by silica gel column chromatography (ethyl acetate : hexane = 1:10) afforded compound **3a** (3.63 g, yield 92%).

The synthesis of 2-(((2-(benzyloxy)naphthalen-1-yl)methyl)amino)-1-phenylethan-1-ol (DC_C01). A mixture of intermediate **3a** (131 mg, 0.5 mmol), 2-amino-1-phenylethan-1-ol **4a** (82 mg, 0.6 mmol), NaBH(OAc)₃ (318 mg, 1.5 mmol), CH₃COOH (57 μ L, 0.5 mmol) was stirred in dry DCE at room temperature for 2.5 h. The resulting mixture was then diluted with water and extracted with DCM. The combined organic layers were washed with brine, dried over anhydrous Na₂SO₄ and filtered. The solvent was evaporated under reduced pressure to give the residue, which was purified by silica gel column chromatography (DCM: CH₃OH = 30:1) to give the product **DC_C01** as a yellow solid (174 mg, yield 91%). ¹H NMR (400 MHz, CDCl₃) δ 8.08 (d, J = 8.8 Hz, 1H), 7.82 (t, J = 8.0 Hz, 2H), 7.55 (t, J = 7.2 Hz, 1H), 7.44 (t, J = 6.8 Hz, 2H), 7.41 (d, J = 4.8 Hz, 2H), 7.39 – 7.35 (m, 2H), 7.34 (d, J = 4.0 Hz, 5H), 7.28 (q, J = 4.4 Hz, 1H), 5.25 (s, 2H), 4.73 (dd, J = 9.2, 3.6 Hz, 1H), 4.37 (q, J = 12.4 Hz, 2H), 2.87 (ddd, J = 21.6, 12.4, 6.4 Hz, 2H). ¹³C NMR (125 MHz, CDCl₃) δ 153.7, 142.1, 136.6, 132.8, 128.9, 128.8, 128.2, 128.1, 127.8, 127.6, 126.9, 126.9, 126.4, 125.4, 123.2, 122.6, 121.1, 114.2, 71.1, 70.9, 56.2, 42.3. HRMS (ESI, positive) m/z calcd for C₂₆H₂₅NO₂ [M + H]⁺: 384.1958. Found: 384.1963.

1-phenyl-2-(((2-(pyridin-4-ylmethoxy)naphthalen-1-yl)methyl)amino)ethan-1-ol (DC_C02). The title compound was synthesized from 2-(pyridin-4-ylmethoxy)-1-naphthaldehyde **3b** (131 mg, 0.5 mmol), 2-amino-1-phenylethan-1-ol **4a** (82 mg, 0.6 mmol), NaBH(OAc)₃ (318 mg, 1.5 mmol), CH₃COOH (57 μ L, 0.5 mmol) in dry DCE (15 mL) according to synthetic procedure for **DC_C01**. The product **DC_C02** is a yellow solid (156 mg, 85% yield). ¹H NMR (400 MHz, CDCl₃) δ 8.62 (d, J = 6.0 Hz, 2H), 8.07 (d, J = 8.4 Hz, 1H),

7.79 (d, $J = 9.2$ Hz, 2H), 7.59 – 7.54 (m, 1H), 7.60 – 7.53 (m, 1H), 7.41 (d, $J = 7.6$ Hz, 1H), 7.37 (d, $J = 6.0$ Hz, 2H), 7.34 – 7.26 (m, 5H), 7.20 (d, $J = 9.0$ Hz, 1H), 5.29 (s, 2H), 4.85 (dd, $J = 9.6, 3.0$ Hz, 1H), 3.50 (s, 2H), 3.29 (s, 2H), 3.10 (dd, $J = 12.0, 3.0$ Hz, 1H), 2.84 (dd, $J = 12.0, 9.6$ Hz, 1H). ^{13}C NMR (125 MHz, DMSO- d_6) δ 154.3, 150.2, 146.8, 144.3, 133.4, 130.1, 129.4, 128.8, 128.5, 127.5, 127.3, 126.4, 124.2, 124.0, 122.3, 115.0, 71.1, 69.1, 57.0, 42.6. HRMS (ESI, positive) m/z calcd for $\text{C}_{25}\text{H}_{24}\text{N}_2\text{O}_2$ [$M + H$] $^+$: 385.1902. Found: 384.1911.

2-(((2-phenethoxynaphthalen-1-yl)methyl)amino)-1-phenylethan-1-ol (DC_C03). The title compound was synthesized from 2-phenethoxy-1-naphthaldehyde **3c** (138 mg, 0.5 mmol), 2-amino-1-phenylethan-1-ol **4a** (82 mg, 0.6 mmol), NaBH(OAc) $_3$ (318 mg, 1.5 mmol), CH $_3$ COOH (57 μL , 0.5 mmol) in dry DCE (15 mL) according to synthetic procedure for **DC_C01**. The product **DC_C03** is a yellow solid (163 mg, 85% yield). ^1H NMR (400 MHz, CDCl $_3$) δ 7.99 (d, $J = 8.8$ Hz, 1H), 7.81 (t, $J = 8.8$ Hz, 2H), 7.56 – 7.51 (m, 1H), 7.40 – 7.35 (m, 2H), 7.33 (d, $J = 3.6$ Hz, 3H), 7.29 (ddd, $J = 8.4, 6.4, 2.0$ Hz, 7H), 4.83 (dd, $J = 9.6, 3.2$ Hz, 1H), 4.68 (s, 2H), 4.42 – 4.37 (m, 2H), 4.33 (t, $J = 10.6$ Hz, 2H), 3.16 (t, $J = 6.8$ Hz, 2H), 3.00 (dd, $J = 12.2, 3.2$ Hz, 1H), 2.70 (dd, $J = 12.0, 9.6$ Hz, 1H). ^{13}C NMR (125 MHz, CDCl $_3$) δ 156.2, 143.2, 139.5, 134.5, 131.7, 130.5, 130.4, 130.1, 129.8, 128.9, 128.8, 128.2, 127.2, 125.2, 123.9, 118.7, 114.9, 71.8, 71.2, 56.6, 43.7, 37.4. HRMS (ESI, positive) m/z calcd for $\text{C}_{27}\text{H}_{27}\text{NO}_2$ [$M + H$] $^+$: 398.2115. Found: 398.2118.

2-(((2-((4-fluorobenzyl)oxy)naphthalen-1-yl)methyl)amino)-1-phenylethan-1-ol (DC_C05). The title compound was synthesized from 2-((4-fluorobenzyl)oxy)-1-naphthaldehyde **3d** (140 mg, 0.5 mmol), 2-amino-1-phenylethan-1-ol **4a** (82 mg, 0.6 mmol), NaBH(OAc) $_3$ (318 mg, 1.5 mmol), CH $_3$ COOH (57 μL , 0.5 mmol) in dry DCE (15 mL) according to synthetic procedure for **DC_C01**. The product **DC_C05** is a white solid (188 mg, 94% yield). ^1H NMR (400 MHz, CDCl $_3$) δ 8.09 (d, $J = 8.4$ Hz, 1H), 7.80 (d, $J = 9.2$ Hz, 1H), 7.71 (d, $J = 8.0$ Hz, 1H), 7.56 (t, $J = 7.6$ Hz, 1H), 7.47 (dd, $J = 8.4, 5.2$ Hz, 2H), 7.37 – 7.32 (m, 1H), 7.29 (dd, $J = 6.4, 2.8$ Hz, 4H), 7.18 (dd, $J = 6.4, 2.4$ Hz, 2H), 7.06 (t, $J = 8.4$ Hz, 2H), 5.51 (s, 2H), 5.31 (s, 2H), 4.99 (d, $J = 8.4$ Hz, 1H), 4.62 (dd, $J = 29.6, 13.2$ Hz, 2H), 3.02 (ddd, $J = 22.4, 12.0, 6.4$ Hz, 2H). ^{13}C NMR (125 MHz, CDCl $_3$) δ 165.1, 163.1, 156.8, 141.7, 134.1, 133.6, 133.5, 133.4, 131.3, 131.2, 130.4, 130.2, 129.8, 129.5, 129.2, 127.2, 125.6, 123.7, 117.3, 117.1, 114.6, 113.5, 71.8, 70.2, 56.5, 43.6. HRMS (ESI, positive) m/z calcd for $\text{C}_{26}\text{H}_{24}\text{FNO}_2$ [$M + H$] $^+$: 402.1805. Found: 402.1809.

2-(((2-((4-chlorobenzyl)oxy)naphthalen-1-yl)methyl)amino)-1-phenylethan-1-ol (DC_C06). The title compound was synthesized from 2-((4-chlorobenzyl)oxy)-1-naphthaldehyde **3e** (148 mg, 0.5 mmol), 2-amino-1-phenylethan-1-ol **4a** (82 mg, 0.6 mmol), NaBH(OAc) $_3$ (318 mg, 1.5 mmol), CH $_3$ COOH (57 μL , 0.5 mmol) in dry DCE (15 mL) according to synthetic procedure for **DC_C01**. The product **DC_C06** is a white solid (200 mg, 96% yield). ^1H NMR (400 MHz, CDCl $_3$) δ 8.05 (d, $J = 8.4$ Hz, 1H), 7.81 (d, $J = 9.2$ Hz, 2H), 7.55 (ddd, $J = 8.4, 6.8, 1.2$ Hz, 1H), 7.42 – 7.37 (m, 1H), 7.35 (d, $J = 4.0$ Hz, 4H), 7.34 – 7.32 (m, 1H), 7.30 (dd, $J = 7.2, 4.0$ Hz, 4H), 7.27 (d, $J = 1.7$ Hz, 1H), 5.19 (s, 2H), 4.80 (dd, $J = 9.2, 3.2$ Hz, 1H), 4.52 (s, 2H), 4.41 (dd, $J = 26.4, 12.8$ Hz, 2H), 2.90 (ddd, $J = 21.6, 12.0, 6.4$ Hz, 2H). ^{13}C NMR (125 MHz, CDCl $_3$) δ 153.7, 141.7, 134.9, 133.5, 132.7, 129.3,

128.9, 128.4, 128.3, 128.2, 127.9, 127.0, 126.7, 125.3, 123.4, 122.4, 119.6, 113.8, 70.7, 70.1, 55.8, 42.1. HRMS (ESI, positive) m/z calcd for $\text{C}_{26}\text{H}_{24}\text{ClNO}_2$ [$M + H$] $^+$: 418.1615. Found: 418.1618.

4-(((1-(((2-hydroxy-2-phenylethyl)amino)methyl)naphthalen-2-yl)oxy)methyl) benzonitrile (DC_C07). The title compound was synthesized from 4-(((1-formylnaphthalen-2-yl)oxy)methyl) benzonitrile **3f** (144 mg, 0.5 mmol), 2-amino-1-phenylethan-1-ol **4a** (82 mg, 0.6 mmol), NaBH(OAc) $_3$ (318 mg, 1.5 mmol), CH $_3$ COOH (57 μL , 0.5 mmol) in dry DCE (15 mL) according to synthetic procedure for **DC_C01**. The product **DC_C07** is a white solid (186 mg, 91% yield). ^1H NMR (400 MHz, CDCl $_3$) δ 8.06 (d, $J = 8.4$ Hz, 1H), 7.82 – 7.76 (m, 2H), 7.67 (d, $J = 8.0$ Hz, 2H), 7.59 – 7.54 (m, 3H), 7.42 – 7.37 (m, 1H), 7.31 (dt, $J = 6.8, 5.2$ Hz, 4H), 7.25 – 7.19 (m, 2H), 5.33 (s, 2H), 4.84 (d, $J = 2.8$ Hz, 1H), 4.49 (dd, $J = 31.6, 13.2$ Hz, 2H), 4.23 (s, 2H), 3.09 (dd, $J = 12.0, 3.2$ Hz, 1H), 2.83 (dd, $J = 12.0, 9.6$ Hz, 1H). ^{13}C NMR (125 MHz, CDCl $_3$) δ 155.5, 143.7, 143.3, 134.5, 134.0, 131.7, 131.0, 130.9, 130.2, 129.9, 129.1, 129.0, 127.2, 125.6, 124.2, 120.3, 120.1, 116.9, 115.2, 113.4, 72.3, 71.6, 57.6, 44.0. HRMS (ESI, positive) m/z calcd for $\text{C}_{27}\text{H}_{24}\text{N}_2\text{O}_2$ [$M + H$] $^+$: 409.1906. Found: 409.1908.

N-((2-(benzyloxy)naphthalen-1-yl)methyl)-2-phenylethan-1-amine (DC_C08). The title compound was synthesized from **3a** (144 mg, 0.5 mmol), 2-phenylethan-1-amine **4b** (73 mg, 0.6 mmol), NaBH(OAc) $_3$ (318 mg, 1.5 mmol), CH $_3$ COOH (57 μL , 0.5 mmol) in dry DCE (15 mL) according to synthetic procedure for **DC_C01**. The product **DC_C08** is a yellow solid (173 mg, 94% yield). ^1H NMR (400 MHz, CDCl $_3$) δ 8.11 (d, $J = 8.4$ Hz, 1H), 7.78 (d, $J = 9.2$ Hz, 1H), 7.66 (d, $J = 8.0$ Hz, 1H), 7.59 – 7.53 (m, 1H), 7.44 – 7.40 (m, 2H), 7.39 – 7.32 (m, 4H), 7.29 (t, $J = 5.2$ Hz, 2H), 7.23 – 7.21 (m, 2H), 6.98 (dd, $J = 7.2, 2.0$ Hz, 2H), 5.26 (s, 2H), 4.53 (s, 2H), 3.04 – 2.97 (m, 2H), 2.93 – 2.88 (m, 2H). ^{13}C NMR (125 MHz, CDCl $_3$) δ 156.9, 138.7, 137.9, 134.2, 133.0, 130.3, 130.2, 130.1, 130.0, 129.7, 129.3, 129.2, 128.1, 125.5, 124.2, 114.8, 114.3, 72.4, 49.8, 42.9, 34.0. HRMS (ESI, positive) m/z calcd for $\text{C}_{26}\text{H}_{25}\text{NO}$ [$M + H$] $^+$: 368.1911. Found: 368.1914.

N-((2-(benzyloxy)naphthalen-1-yl)methyl)-2-(pyridin-2-yl)ethan-1-amine (DC_C09). The title compound was synthesized from **3a** (144 mg, 0.5 mmol), 2-(pyridin-2-yl)ethan-1-amine **4c** (73 mg, 0.6 mmol), NaBH(OAc) $_3$ (318 mg, 1.5 mmol), CH $_3$ COOH (57 μL , 0.5 mmol) in dry DCE (15 mL) according to synthetic procedure for **DC_C01**. The product **DC_C09** is a yellow solid (171 mg, 93% yield). ^1H NMR (400 MHz, CDCl $_3$) δ 8.09 (d, $J = 8.8$ Hz, 1H), 7.87 (d, $J = 9.2$ Hz, 1H), 7.81 (d, $J = 8.0$ Hz, 1H), 7.71 (d, $J = 4.8$ Hz, 1H), 7.65 (t, $J = 7.6$ Hz, 1H), 7.50 (td, $J = 7.6, 1.6$ Hz, 1H), 7.44 – 7.38 (m, 4H), 7.36 (d, $J = 2.4$ Hz, 1H), 7.35 – 7.31 (m, 2H), 7.05 – 6.91 (m, 2H), 5.32 (s, 2H), 4.79 (s, 2H), 3.34 – 3.29 (m, 2H), 3.29 – 3.24 (m, 2H). ^{13}C NMR (125 MHz, CDCl $_3$) δ 159.1, 156.2, 148.5, 137.9, 136.8, 133.6, 132.7, 129.8, 129.7, 129.6, 129.2, 128.9, 128.0, 125.0, 124.1, 122.8, 122.7, 114.4, 112.7, 72.0, 46.4, 42.0, 31.6. HRMS (ESI, positive) m/z calcd for $\text{C}_{25}\text{H}_{24}\text{N}_2\text{O}$ [$M + H$] $^+$: 369.2013. Found: 369.2017.

N-((2-(benzyloxy)naphthalen-1-yl)methyl)-2-(1H-indol-3-yl)ethan-1-amine (DC_C10). The title compound was synthesized from **3a** (144 mg, 0.5 mmol), 2-(1H-indol-3-yl)ethan-1-amine **4d** (96 mg, 0.6 mmol), NaBH(OAc) $_3$ (318 mg, 1.5 mmol), CH $_3$ COOH (57 μL , 0.5 mmol) in dry DCE (15 mL) according to synthetic procedure for **DC_C01**.

The product **DC_C10** is a yellow solid (183 mg, 90% yield). ^1H NMR (400 MHz, DMSO- d_6) δ 10.99 (s, 1H), 8.93 (s, 1H), 8.20 (d, J = 8.4 Hz, 1H), 8.09 (d, J = 9.2 Hz, 1H), 7.96 (d, J = 8.0 Hz, 1H), 7.66 – 7.60 (m, 2H), 7.55 (dd, J = 7.6, 1.6 Hz, 2H), 7.51 (d, J = 8.0 Hz, 1H), 7.46 (t, J = 7.2 Hz, 1H), 7.40 – 7.35 (m, 2H), 7.34 (t, J = 3.8 Hz, 2H), 7.18 (d, J = 2.3 Hz, 1H), 7.14 – 7.09 (m, 1H), 7.04 – 6.99 (m, 1H), 5.37 (s, 2H), 4.68 (s, 2H), 3.29 – 3.24 (m, 2H), 3.13 – 3.08 (m, 2H). ^{13}C NMR (125 MHz, CDCl_3) δ 154.5, 136.1, 135.4, 132.2, 131.3, 128.4, 128.3, 128.2, 127.8, 127.7, 126.6, 125.8, 123.8, 123.7, 121.7, 121.4, 119.1, 117.7, 112.6, 111.2, 110.5, 108.2, 69.7, 45.1, 41.3, 22.0. HRMS (ESI, positive) m/z calcd for $\text{C}_{28}\text{H}_{26}\text{N}_2\text{O}$ $[\text{M} + \text{H}]^+$: 407.2101. Found: 407.2103.

N-((2-(benzyloxy)naphthalen-1-yl)methyl)-2-(piperidin-1-yl)ethan-1-amine (DC_C11). The title compound was synthesized from **3a** (144 mg, 0.5 mmol), 2-(piperidin-1-yl)ethan-1-amine **4e** (77 mg, 0.6 mmol), $\text{NaBH}(\text{OAc})_3$ (318 mg, 1.5 mmol), CH_3COOH (57 μL , 0.5 mmol) in dry DCE (15 mL) according to synthetic procedure for **DC_C01**. The product **DC_C11** is a yellow solid (161 mg, 86% yield). ^1H NMR (400 MHz, CDCl_3) δ 8.00 (t, J = 8.8 Hz, 1H), 7.92 (d, J = 9.2 Hz, 1H), 7.85 (d, J = 8.0 Hz, 1H), 7.65 – 7.60 (m, 1H), 7.45 (t, J = 7.2 Hz, 3H), 7.43 – 7.39 (m, 2H), 7.38 (t, J = 3.2 Hz, 1H), 6.95 (d, J = 8.4 Hz, 1H), 5.33 (s, 2H), 4.72 (s, 1H), 4.67 (s, 2H), 3.01 – 2.97 (m, 2H), 2.63 – 2.58 (m, 2H), 2.20 (s, 4H), 1.31 (s, 6H). ^{13}C NMR (125 MHz, CDCl_3) δ 155.1, 136.0, 132.9, 131.6, 129.4, 129.0, 129.0, 128.6, 128.3, 127.6, 124.5, 122.0, 114.4, 113.8, 71.6, 54.1, 53.6, 42.1, 41.3, 24.8, 23.4. HRMS (ESI, positive) m/z calcd for $\text{C}_{25}\text{H}_{30}\text{N}_2\text{O}$ $[\text{M} + \text{H}]^+$: 375.2523. Found: 375.2532.

N-((2-(benzyloxy)naphthalen-1-yl)methyl)-2-morpholinoethan-1-amine (DC_C12). The title compound was synthesized from **3a** (144 mg, 0.5 mmol), 2-morpholinoethan-1-amine **4f** (78 mg, 0.6 mmol), $\text{NaBH}(\text{OAc})_3$ (318 mg, 1.5 mmol), CH_3COOH (57 μL , 0.5 mmol) in dry DCE (15 mL) according to synthetic procedure for **DC_C01**. The product **DC_C12** is a yellow solid (163 mg, 87% yield). ^1H NMR (400 MHz, CDCl_3) δ 8.01 (d, J = 8.4 Hz, 1H), 7.91 (d, J = 9.2 Hz, 1H), 7.82 (d, J = 8.0 Hz, 1H), 7.63 (t, J = 7.8 Hz, 1H), 7.43 (t, J = 7.2 Hz, 5H), 7.38 (t, J = 4.3 Hz, 1H), 7.35 (d, J = 4.8 Hz, 1H), 5.32 (s, 2H), 4.71 (s, 2H), 3.21 (s, 4H), 2.97 – 2.90 (m, 2H), 2.56 – 2.49 (m, 2H), 1.99 (t, J = 4.4 Hz, 4H). ^{13}C NMR (125 MHz, CDCl_3) δ 156.8, 137.1, 134.2, 133.7, 130.6, 130.6, 130.5, 130.3, 130.2, 129.1, 126.2, 123.2, 115.1, 113.8, 73.1, 67.8, 54.8, 54.0, 43.1, 42.5. HRMS (ESI, positive) m/z calcd for $\text{C}_{24}\text{H}_{28}\text{N}_2\text{O}_2$ $[\text{M} + \text{H}]^+$: 377.2354. Found: 377.2361.

N-((2-(benzyloxy)naphthalen-1-yl)methyl)-2-(4-fluorophenyl)ethan-1-amine (DC_C13). The title compound was synthesized from **3a** (144 mg, 0.5 mmol), 2-(4-fluorophenyl)ethan-1-amine **4g** (84 mg, 0.6 mmol), $\text{NaBH}(\text{OAc})_3$ (318 mg, 1.5 mmol), CH_3COOH (57 μL , 0.5 mmol) in dry DCE (15 mL) according to synthetic procedure for **DC_C01**. The product **DC_C13** is a yellow solid (160 mg, 83% yield). ^1H NMR (400 MHz, CDCl_3) δ 8.08 (d, J = 8.8 Hz, 1H), 7.79 (d, J = 9.2 Hz, 1H), 7.69 (d, J = 8.2 Hz, 1H), 7.55 (t, J = 7.6 Hz, 1H), 7.42 (t, J = 8.0 Hz, 2H), 7.40 – 7.34 (m, 3H), 7.34 – 7.29 (m, 2H), 6.91 (p, J = 8.8 Hz, 4H), 5.26 (s, 2H), 4.49 (s, 2H), 2.98 – 2.92 (m, 2H), 2.86 – 2.79 (m, 2H). ^{13}C NMR (125 MHz, CDCl_3) δ 164.1, 162.1, 156.8, 138.0, 134.7, 134.7, 134.2, 132.8, 131.7, 131.6, 130.4, 130.2, 130.0, 129.7, 129.2, 129.1, 125.5, 124.2, 116.8, 116.6, 115.2, 114.9, 72.5, 50.2, 43.2,

33.6. HRMS (ESI, positive) m/z calcd for $\text{C}_{26}\text{H}_{24}\text{FNO}$ $[\text{M} + \text{H}]^+$: 386.1927. Found: 386.1929. DOI: 10.1039/C7OB00070G

4-((2-((2-(benzyloxy)naphthalen-1-yl)methyl)amino)ethyl)phenol (DC_C14). The title compound was synthesized from **3a** (144 mg, 0.5 mmol), 4-(2-aminoethyl)phenol **4h** (82 mg, 0.6 mmol), $\text{NaBH}(\text{OAc})_3$ (318 mg, 1.5 mmol), CH_3COOH (57 μL , 0.5 mmol) in dry DCE (15 mL) according to synthetic procedure for **DC_C01**. The product **DC_C14** is a yellow solid (167 mg, 87% yield). ^1H NMR (400 MHz, DMSO- d_6) δ 8.06 (d, J = 8.9 Hz, 1H), 7.85 (dd, J = 8.5, 3.0 Hz, 2H), 7.48 (dd, J = 14.9, 7.9 Hz, 4H), 7.39 (t, J = 6.8 Hz, 2H), 7.35 (dd, J = 7.1, 3.3 Hz, 2H), 6.93 (d, J = 8.3 Hz, 2H), 6.63 (d, J = 8.3 Hz, 2H), 5.25 (s, 2H), 4.18 (s, 2H), 3.39 (s, 2H), 2.78 (t, J = 7.3 Hz, 2H), 2.59 (t, J = 7.3 Hz, 2H). ^{13}C NMR (125 MHz, DMSO- d_6) δ 172.6, 155.9, 154.3, 137.8, 133.5, 130.6, 129.8, 129.3, 128.9, 128.7, 128.3, 128.0, 126.9, 124.2, 123.9, 121.7, 115.7, 115.5, 71.0, 51.5, 43.0, 35.2, 21.7. HRMS (ESI, positive) m/z calcd for $\text{C}_{26}\text{H}_{25}\text{NO}_2$ $[\text{M} + \text{H}]^+$: 384.1965. Found: 386.1972.

N-((2-(benzyloxy)naphthalen-1-yl)methyl)-2-(p-tolyl)ethan-1-amine (DC_C15). The title compound was synthesized from **3a** (144 mg, 0.5 mmol), 2-(p-tolyl)ethan-1-amine **4i** (81 mg, 0.6 mmol), $\text{NaBH}(\text{OAc})_3$ (318 mg, 1.5 mmol), CH_3COOH (57 μL , 0.5 mmol) in dry DCE (15 mL) according to synthetic procedure for **DC_C01**. The product **DC_C15** is a yellow solid (185 mg, 97% yield). ^1H NMR (400 MHz, CDCl_3) δ 8.08 (d, J = 8.4 Hz, 1H), 7.79 (d, J = 8.8 Hz, 1H), 7.73 (d, J = 8.0 Hz, 1H), 7.54 (t, J = 7.6 Hz, 1H), 7.43 – 7.31 (m, 6H), 7.28 (d, J = 8.4 Hz, 1H), 7.03 (d, J = 7.2 Hz, 2H), 6.92 (d, J = 7.2 Hz, 2H), 5.52 (s, 1H), 5.22 (s, 2H), 4.49 (s, 2H), 2.99 (t, J = 7.6 Hz, 2H), 2.86 (t, J = 7.2 Hz, 2H), 2.31 (s, 3H). ^{13}C NMR (125 MHz, CDCl_3) δ 156.7, 138.1, 137.5, 136.2, 134.4, 132.5, 130.7, 130.5, 130.2, 130.1, 130.0, 129.7, 129.1, 125.4, 124.3, 116.2, 115.1, 72.5, 50.1, 43.1, 34.4, 22.5. HRMS (ESI, positive) m/z calcd for $\text{C}_{27}\text{H}_{27}\text{NO}$ $[\text{M} + \text{H}]^+$: 382.2287. Found: 382.2293.

N-((2-(benzyloxy)naphthalen-1-yl)methyl)-2-(4-chlorophenyl)ethan-1-amine (DC_C16). The title compound was synthesized from **3a** (144 mg, 0.5 mmol), 2-(4-chlorophenyl)ethan-1-amine **4j** (94 mg, 0.6 mmol), $\text{NaBH}(\text{OAc})_3$ (318 mg, 1.5 mmol), CH_3COOH (57 μL , 0.5 mmol) in dry DCE (15 mL) according to synthetic procedure for **DC_C01**. The product **DC_C16** is a yellow solid (191 mg, 95% yield). ^1H NMR (400 MHz, CDCl_3) δ 8.07 (d, J = 8.4 Hz, 1H), 7.79 (d, J = 9.2 Hz, 1H), 7.69 (d, J = 8.4 Hz, 1H), 7.55 (ddd, J = 8.4, 6.8, 1.2 Hz, 1H), 7.43 (dt, J = 5.6, 3.2 Hz, 2H), 7.39 (d, J = 4.0 Hz, 1H), 7.37 (t, J = 1.6 Hz, 1H), 7.35 (d, J = 5.6 Hz, 1H), 7.29 (d, J = 7.2 Hz, 2H), 7.20 – 7.15 (m, 2H), 6.89 (d, J = 8.4 Hz, 2H), 5.25 (s, 2H), 4.48 (s, 2H), 2.97 – 2.91 (m, 2H), 2.83 – 2.77 (m, 2H). ^{13}C NMR (125 MHz, DMSO- d_6) δ 155.1, 137.0, 136.9, 132.6, 131.1, 131.0, 130.4, 128.6, 128.5, 128.4, 128.0, 127.9, 127.1, 123.8, 123.2, 114.5, 70.4, 48.6, 41.0, 31.6. HRMS (ESI, positive) m/z calcd for $\text{C}_{26}\text{H}_{24}\text{ClNO}$ $[\text{M} + \text{H}]^+$: 402.1852. Found: 402.1874.

N-((2-(benzyloxy)naphthalen-1-yl)methyl)-2-(3-fluorophenyl)ethan-1-amine (DC_C17). The title compound was synthesized from **3a** (144 mg, 0.5 mmol), 2-(3-fluorophenyl)ethan-1-amine **4k** (84 mg, 0.6 mmol), $\text{NaBH}(\text{OAc})_3$ (318 mg, 1.5 mmol), CH_3COOH (57 μL , 0.5 mmol) in dry DCE (15 mL) according to synthetic procedure for **DC_C01**. The product **DC_C17** is a yellow solid (175 mg, 91% yield).

^1H NMR (400 MHz, CDCl_3) δ 8.09 (d, J = 8.4 Hz, 1H), 7.78 (d, J = 9.2 Hz, 1H), 7.68 (d, J = 8.0 Hz, 1H), 7.54 (ddd, J = 8.4, 6.8, 1.2 Hz, 1H), 7.45 (dd, J = 7.6, 1.6 Hz, 2H), 7.41 – 7.34 (m, 3H), 7.32 (t, J = 3.6 Hz, 1H), 7.30 (s, 1H), 7.18 (td, J = 8.0, 6.0 Hz, 1H), 6.89 (td, J = 8.4, 2.4 Hz, 1H), 6.78 (d, J = 7.6 Hz, 1H), 6.70 – 6.65 (m, 1H), 5.28 (s, 2H), 4.90 (s, 1H), 4.46 (s, 2H), 2.98 – 2.93 (m, 2H), 2.85 – 2.78 (m, 2H). ^{13}C NMR (125 MHz, CDCl_3) δ 165.2, 163.3, 156.8, 141.9, 141.9, 138.1, 134.3, 132.6, 131.4, 131.3, 130.4, 130.2, 130.0, 129.8, 129.3, 129.1, 125.9, 125.8, 125.4, 124.3, 117.1, 117.0, 116.0, 115.1, 115.0, 114.8, 72.5, 50.1, 43.3, 34.4. HRMS (ESI, positive) m/z calcd for $\text{C}_{26}\text{H}_{24}\text{FNO}$ [$\text{M} + \text{H}$] $^+$: 386.1946. Found: 386.1972.

N-((2-(benzyloxy)naphthalen-1-yl)methyl)-N-methyl-2-phenylethan-1-amine (DC_C18). The title compound was synthesized from **3a** (144 mg, 0.5 mmol), N-methyl-2-phenylethan-1-amine **4l** (81 mg, 0.6 mmol), $\text{NaBH}(\text{OAc})_3$ (318 mg, 1.5 mmol), CH_3COOH (57 μL , 0.5 mmol) in dry DCE (15 mL) according to synthetic procedure for **DC_C01**. The product **DC_C18** is a yellow solid (183 mg, 96% yield). ^1H NMR (400 MHz, CDCl_3) δ 8.19 (d, J = 8.4 Hz, 1H), 7.92 (d, J = 8.8 Hz, 1H), 7.83 (d, J = 8.0 Hz, 1H), 7.60 (t, J = 8.0 Hz, 1H), 7.46 (t, J = 5.6 Hz, 2H), 7.43 – 7.34 (m, 5H), 7.29 (t, J = 7.2 Hz, 2H), 7.27 – 7.22 (m, 1H), 7.14 (d, J = 6.8 Hz, 2H), 5.31 (s, 2H), 4.57 (s, 2H), 3.14 (s, 4H), 2.58 (s, 3H). ^{13}C NMR (125 MHz, CDCl_3) δ 155.4, 135.9, 132.5, 132.2, 129.3, 129.0, 128.7, 128.6, 127.7, 124.8, 122.3, 114.0, 113.2, 71.9, 66.0, 53.2, 41.1, 20.9. HRMS (ESI, positive) m/z calcd for $\text{C}_{27}\text{H}_{27}\text{NO}$ [$\text{M} + \text{H}$] $^+$: 382.2351. Found: 382.2367.

1-formylnaphthalen-2-yl benzoate (3g). To a solution of benzoyl chloride **2g** (1.23 g, 8.70 mmol) in dry THF (10 mL) was added dropwise to a mixture of 2-hydroxynaphthaldehyde **1a** (1.0 g, 5.81 mmol) and K_2CO_3 (1.2 g, 8.70 mmol) in THF (40 mL) at 0°C and under nitrogen atmosphere. The reaction mixture was warmed to room temperature and stirred vigorously for 16 h. The mixture was poured into water (40 mL) and extracted with ethyl acetate (3 \times 50 mL). The combined organic phases were washed with brine (100 mL), dried (Na_2SO_4), and evaporated in vacuo. The crude product thus obtained was purified through column chromatography over silica using methylene chloride: hexanes (1:1) mixture to afford 1.2 g (75%) of **3g** as a white solid.

1-(((2-hydroxy-2-phenylethyl)amino)methyl)naphthalen-2-yl benzoate (DC_C04). The title compound was synthesized from **3g** (138 mg, 0.5 mmol), 2-amino-1-phenylethan-1-ol **4a** (82 mg, 0.6 mmol), $\text{NaBH}(\text{OAc})_3$ (318 mg, 1.5 mmol), CH_3COOH (57 μL , 0.5 mmol) in dry DCE (15 mL) according to synthetic procedure for **DC_C01**. The product **DC_C04** is a canary solid (153 mg, yield 77%). ^1H NMR (400 MHz, CDCl_3) δ 8.26 (d, J = 8.8 Hz, 1H), 7.82 (d, J = 9.2 Hz, 2H), 7.79 – 7.75 (m, 2H), 7.47 – 7.35 (m, 8H), 7.33 – 7.29 (m, 2H), 7.24 – 7.20 (m, 3H), 6.95 (s, 1H), 5.47 (dd, J = 49.2, 15.6 Hz, 2H), 5.02 – 4.82 (m, 2H), 3.61 – 3.51 (m, 1H), 3.44 (d, J = 14.0 Hz, 1H). ^{13}C NMR (125 MHz, CDCl_3) δ 156.8, 143.2, 133.2, 132.2, 130.4, 130.1, 130.0, 129.9, 129.7, 129.5, 128.5, 128.4, 128.3, 127.3, 127.0, 124.4, 123.7, 121.4, 75.2, 49.3, 42.6. HRMS (ESI) m/z calcd for $\text{C}_{26}\text{H}_{22}\text{NO}_3$ [$\text{M} - \text{H}$] $^-$: 396.1605. Found: 396.1608.

2-(benzyloxy)benzaldehyde (3h). The title compound was synthesized from 2-hydroxybenzaldehyde **1b** (610 mg, 5.00 mmol), anhydrous K_2CO_3 (2.50 g, 18.00 mmol) and (chloromethyl)benzene

2a (823 mg, 6.00 mmol) and KI (167 mg, 1.00 mmol) in dry acetone (15 mL) according to synthetic procedure for **3a**. The product **3h** is a colorless solid (934 mg, yield 88%).

2-((2-(benzyloxy)benzyl)amino)-1-phenylethan-1-ol (DC_C19). The title compound was synthesized from **3h** (106 mg, 0.5 mmol), 2-amino-1-phenylethan-1-ol **4a** (82 mg, 0.6 mmol), $\text{NaBH}(\text{OAc})_3$ (318 mg, 1.5 mmol), CH_3COOH (57 μL , 0.5 mmol) in dry DCE (15 mL) according to synthetic procedure for **DC_C01**. The product **DC_C19** is a yellow solid (145 mg, 87% yield). ^1H NMR (400 MHz, CDCl_3) δ 7.38 (dt, J = 9.2, 7.2 Hz, 6H), 7.33 – 7.29 (m, 4H), 7.28 – 7.22 (m, 2H), 6.92 (t, J = 7.6 Hz, 2H), 5.15 (s, 2H), 5.01 (d, J = 9.6 Hz, 1H), 4.40 (s, 2H), 4.13 (dd, J = 34.0, 13.2 Hz, 2H), 3.07 (dd, J = 12.0, 2.4 Hz, 1H), 2.83 (dd, J = 12.0, 10.4 Hz, 1H). ^{13}C NMR (125 MHz, CDCl_3) δ 156.3, 142.0, 136.4, 129.9, 128.4, 128.2, 127.8, 127.6, 126.9, 126.8, 126.4, 125.4, 120.4, 111.3, 70.7, 69.6, 55.4, 48.1. HRMS (ESI, positive) m/z calcd for $\text{C}_{22}\text{H}_{23}\text{NO}_2$ [$\text{M} + \text{H}$] $^+$: 334.1824. Found: 386.1846.

Author Contributions

Mingyue Zheng and Cheng Luo conceived and designed the project. Yan Ye and Yulan Wang performed molecular modeling and virtual screening, Bidong Zhang and Yaxi Yang performed chemical syntheses, Ruifeng Mao and Hong Ding performed cellular assays, Chenhua Zhang and Yu-Chih Liu measured enzyme activity and inhibition, Yan Ye and Jing Xing analyzed the data. Yan Ye, Bidong Zhang and Mingyue Zheng wrote the paper. All authors discussed the results and commented on the manuscript. All authors approved the final version of the manuscript.

Acknowledgements

We gratefully acknowledge financial support from the Strategic Priority Research Program of the Chinese Academy of Sciences (XDA12050201 to M.Z.), the National Basic Research Program (2015CB910304 and 2015CB910304 to X.L.), the National Natural Science Foundation of China (21210003 and 81230076 to H.J., 81430084 to K.C. and 81625022 to C.L.), and the National Key Research & Development Plan (2016YF1201003 to M.Z.), and the Fund of State Key Laboratory of Toxicology and Medical Countermeasures, Academy of Military Medical Science (TMC201505 to C.L.).

References

- 1 J. Fuhrmann and P. R. Thompson, *ACS Chem Biol*, 2016, **11**, 654–668.
- 2 P. Aggarwal, L. P. Vaites, J. K. Kim, H. Mellert, B. Gurung, H. Nakagawa, M. Herlyn, X. Hua, A. K. Rustgi, S. B. McMahon and J. A. Diehl, *Cancer Cell*, 2010, **18**, 329–340.
- 3 M. T. Bedford and S. Richard, *Mol Cell*, 2005, **18**, 263–272.
- 4 M. Jansson, S. T. Durant, E. C. Cho, S. Sheahan, M. Edelmann, B. Kessler and N. B. La Thangue, *Nat Cell Biol*, 2008, **10**, 1431–1439.
- 5 A. Scoumanne, J. Zhang and X. Chen, *Nucleic Acids Res*, 2009, **37**, 4965–4976.

- 6 Q. Zhao, G. Rank, Y. T. Tan, H. Li, R. L. Moritz, R. J. Simpson, L. Cerruti, D. J. Curtis, D. J. Patel, C. D. Allis, J. M. Cunningham and S. M. Jane, *Nat Struct Mol Biol*, 2009, **16**, 304-311.
- 7 W. W. Tee, M. Pardo, T. W. Theunissen, L. Yu, J. S. Choudhary, P. Hajkova and M. A. Surani, *Genes Dev*, 2010, **24**, 2772-2777.
- 8 A. Moretting, R. M. Baldwin and J. Cote, *Mutagenesis*, 2015, **30**, 177-189.
- 9 S. S. Wolf, *Cell Mol Life Sci*, 2009, **66**, 2109-2121.
- 10 Y. Yang, A. Hadjikyriacou and Z. Xia, *Nat Commun*, 2015, **6**, 6428.
- 11 C. I. Zurita-Lopez, T. Sandberg, R. Kelly and S. G. Clarke, *J Biol Chem*, 2012, **287**, 7859-7870.
- 12 S. Pal, S. N. Vishwanath, H. Erdjument-Bromage, P. Tempst and S. Sif, *Mol Cell Biol*, 2004, **24**, 9630-9645.
- 13 S. Pal, R. A. Baiocchi, J. C. Byrd, M. R. Grever, S. T. Jacob and S. Sif, *Embo j*, 2007, **26**, 3558-3569.
- 14 E. S. Burgos, C. Wilczek, T. Onikubo, J. B. Bonanno, J. Jansong, U. Reimer and D. Shechter, *J Biol Chem*, 2015, **290**, 9674-9689.
- 15 Z. Gu, S. Gao, F. Zhang, Z. Wang, W. Ma, R. E. Davis and Z. Wang, *Biochem J*, 2012, **446**, 235-241.
- 16 M. A. Powers, M. M. Fay, R. E. Factor, A. L. Welm and K. S. Ullman, *Cancer Res*, 2011, **71**, 5579-5587.
- 17 B. Zhang, S. Dong, R. Zhu, C. Hu, J. Hou, Y. Li, Q. Zhao, X. Shao, Q. Bu, H. Li, Y. Wu, X. Cen and Y. Zhao, *Oncotarget*, 2015, **6**, 22799-22811.
- 18 L. Alinari, K. V. Mahasenan, F. Yan, V. Karkhanis, J. H. Chung, E. M. Smith, C. Quinion, P. L. Smith, L. Kim, J. T. Patton, R. Lapalombella, B. Yu, Y. Wu, S. Roy, A. De Leo, S. Pileri, C. Agostinelli, L. Ayers, J. E. Bradner, S. Chen-Kiang, O. Elemento, T. Motiwala, S. Majumder, J. C. Byrd, S. Jacob, S. Sif, C. Li and R. A. Baiocchi, *Blood*, 2015, **125**, 2530-2543.
- 19 H. C. Nguyen, M. Wang, A. Salsburg and B. Knuckley, *ACS Comb Sci*, 2015, **17**, 500-505.
- 20 M. B. Dillon, D. A. Bachovchin, S. J. Brown, M. G. Finn, H. Rosen, B. F. Cravatt and K. A. Mowen, *ACS Chem Biol*, 2012, **7**, 1198-1204.
- 21 J. Wu, N. Xie, Y. Feng and Y. G. Zheng, *J Biomol Screen*, 2012, **17**, 237-244.
- 22 Y. Feng, M. Li, B. Wang and Y. G. Zheng, *J Med Chem*, 2010, **53**, 6028-6039.
- 23 A. Spannhoff, R. Heinke, I. Bauer, P. Trojer, E. Metzger, R. Gust, R. Schule, G. Brosch, W. Sippl and M. Jung, *J Med Chem*, 2007, **50**, 2319-2325.
- 24 E. Chan-Penebre, K. G. Kuplast, C. R. Majer, P. A. Boriack-Sjodin, T. J. Wigle, L. D. Johnston, N. Rioux, M. J. Munchhof, L. Jin, S. L. Jacques, K. A. West, T. Lingaraj, K. Stickland, S. A. Ribich, A. Raimondi, M. P. Scott, N. J. Waters, R. M. Pollock, J. J. Smith, O. Barbash, M. Pappalardi, T. F. Ho, K. Nurse, K. P. Oza, K. T. Gallagher, R. Kruger, M. P. Moyer, R. A. Copeland, R. Chesworth and K. W. Duncan, *Nat Chem Biol*, 2015, **11**, 432-437.
- 25 ClinicalTrials.gov, <https://clinicaltrials.gov/ct2/show/NCT02783300>, (accessed April 11, 2016).
- 26 S. Kannan, J. Melesina, A. T. Hauser, A. Chakrabarti, T. Heimbürg, K. Schmidtkunz, A. Walter, M. Marek, R. J. Pierce, C. Romier, M. Jung and W. Sippl, *J Chem Inf Model*, 2014, **54**, 3005-3019.
- 27 G. B. Li, L. L. Yang, Y. Yuan, J. Zou, Y. Cao, S. Y. Yang, R. Xiang and M. Xiang, *Methods*, 2015, **71**, 158-166.
- 28 S. Chen, Y. Wang, W. Zhou, S. Li, J. Peng, Z. Shi, J. Hu, Y. C. Liu, H. Ding, Y. Lin, L. Li, S. Cheng, J. Liu, T. Lu, H. Jiang, B. Liu, M. Zheng and C. Luo, *J Med Chem*, 2014, **57**, 9028-9041.
- 29 F. Meng, S. Cheng, H. Ding, S. Liu, Y. Liu, K. Zhu, S. Chen, J. Lu, Y. Xie, L. Li, R. Liu, Z. Shi, Y. Zhou, Y. C. Liu, M. Zheng, H. Jiang, W. Lu, H. Liu and C. Luo, *J Med Chem*, 2015, **58**, 8166-8181.
- 30 J. Wang, L. Chen, S. H. Sinha, Z. Liang, H. Chai, S. Muniyan, Y. W. Chou, C. Yang, L. Yan, Y. Feng, K. K. Li, M. F. Lin, H. Liang, Y. G. Zheng and C. Luo, *J Med Chem*, 2012, **55**, 7978-7987.
- 31 K. W. Duncan, N. Rioux, P. A. Boriack-Sjodin, M. J. Munchhof, L. A. Reiter, C. R. Majer, L. Jin, L. D. Johnston, E. Chan-Penebre, K. G. Kuplast, M. Porter Scott, R. M. Pollock, N. J. Waters, J. J. Smith, M. P. Moyer, R. A. Copeland and R. Chesworth, *ACS Med Chem Lett*, 2016, **7**, 162-166.
- 32 A. Cereto-Massague, L. Guasch, C. Valls, M. Mulero, G. Pujadas and S. Garcia-Vallve, *Bioinformatics*, 2012, **28**, 1661-1662.
- 33 J. B. Baell and G. A. Holloway, *J Med Chem*, 2010, **53**, 2719-2740.
- 34 L. Sun, M. Wang, Z. Lv, N. Yang, Y. Liu, S. Bao, W. Gong and R. M. Xu, *Proc Natl Acad Sci U S A*, 2011, **108**, 20538-20543.
- 35 K. J. Duffy, M. G. Darcy, E. Delorme, S. B. Dillon, D. F. Eppley, C. Erickson-Miller, L. Giampa, C. B. Hopson, Y. Huang, R. M. Keenan, P. Lamb, L. Leong, N. Liu, S. G. Miller, A. T. Price, J. Rosen, R. Shah, T. N. Shaw, H. Smith, K. C. Stark, S. S. Tian, C. Tyree, K. J. Wiggall, L. Zhang and J. I. Luengo, *J Med Chem*, 2001, **44**, 3730-3745.
- 36 D. Koszelewski, I. Lavandera, D. Clay, G. M. Guebitz, D. Rozzell and W. Kroutil, *Angew Chem Int Ed Engl*, 2008, **47**, 9337-9340.
- 37 E. M. Billaud, A. Vidal, A. Vincenot, S. Besse, B. Bouchon, E. Debiton, E. Miot-Noirault, I. Miladi, L. Rbah-Vidal, P. Auzeloux and J. M. Chezal, *ACS Med Chem Lett*, 2015, **6**, 168-172.
- 38 A. F. Abdel-Magid, K. G. Carson, B. D. Harris, C. A. Maryanoff and R. D. Shah, *J Org Chem*, 1996, **61**, 3849-3862.
- 39 H. S. Huang, J. F. Chiou, Y. Fong, C. C. Hou, Y. C. Lu, J. Y. Wang, J. W. Shih, Y. R. Pan and J. J. Lin, *J Med Chem*, 2003, **46**, 3300-3307.
- 40 J. Chung, V. Karkhanis, S. Tae, F. Yan, P. Smith, L. W. Ayers, C. Agostinelli, S. Pileri, G. V. Denis, R. A. Baiocchi and S. Sif, *J Biol Chem*, 2013, **288**, 35534-35547.
- 41 L. Wang, S. Pal and S. Sif, *Mol Cell Biol*, 2008, **28**, 6262-6277.